

# Image Reconstruction Based on Deterministic and Heuristic Approach

Tibor BACHOREC, Jarmila DĚDKOVÁ

Dept. of Theoretical and Experimental Electrical Engineering, Brno University of Technology  
Kolejní 2906/4, 612 00 Brno, Czech Republic  
bachorec@feec.vutbr.cz, dedkova@feec.vutbr.cz

**Abstract.** *The aim of this paper is to provide a survey of the recent development in new algorithms and techniques to solve the electrical impedance tomography (EIT) inverse problem. The EIT problem is nonlinear and ill-posed. The modified Newton-Raphson method with the Tikhonov regularization and the differential evolution algorithm are used to obtain high-quality reconstruction in EIT problems. Numerical results of the reconstruction based on both deterministic and heuristic methods are presented and compared. Finally, we provide recommendations of solutions of still open problems in this field.*

## Keywords

Deterministic method, heuristic approach, inverse problem, regularization, differential evolution algorithm.

## 1. Introduction

Electrical impedance tomography is a widely investigated problem with many applications in physical and biological sciences. Geophysical imaging is used for finding underground conducting fluid plumes near the surface and obtaining information about rock porosity or fracture formation. Another application of EIT is for example in non-destructive testing and identification of material defects like cracks, or identification of corrosion in production materials. Medical imaging can be used primarily for detection of pulmonary emboli, non-invasive monitoring of heart function and blood flow, and for breast cancer detection.

The theoretical background of EIT is given in [1]. The basic principle of EIT is very simple. The currents are applied through the electrodes attached to the surface of the object and the resulting voltages are measured using the same or additional electrodes. Internal impedivity distribution is recalculated from the measured voltages and currents. It is well known that while the forward problem is well-posed, the inverse problem is highly ill-posed. Various numerical techniques with different advantages have been developed to solve this problem. The aim is to reconstruct, as accurately and fast as possible, the impedivity distribution in two or three dimensional models.

So the EIT image reconstruction problem is an ill-posed inverse problem of finding such internal impedivity distribution that minimizes certain optimization criteria. The optimization necessitates algorithms that impose regularization and some prior information constraint. The regularization techniques vary in their complexity. This paper proposes new variants of the regularization techniques to be used for the acquirement of more accurate reconstruction results and the possibility of applying the differential evolution algorithm in an optimization process.

## 2. Forward and Inverse Problem

EIT is used to reconstruct the impedivity distribution by the measured surface electric potential distribution around the phantom when injecting current into the object. Usually, a set of voltage measurements is acquired from the boundaries of the determined volume, whilst it is subjected to a sequence of low-frequency current patterns. In principle, measuring both the amplitude and the phase angle of the voltage can result in images of electric conductivity and permittivity in the interior of the model. Alternating current patterns are preferred to direct current ones to avoid polarization effects. Since the frequency of the injected current is sufficiently low, usually in the range of 10-100 kHz, EIT can be treated as a quasi-static problem. So we only consider the conductivity for simplicity. The scalar potential  $U$  can be therefore introduced, and so the resulting field is conservative and the continuity equation for the volume current density can be expressed by the potential  $U$ :

$$\operatorname{div}(\sigma \operatorname{grad} U) = 0 \quad . \quad (1)$$

Equation (1) together with the modified complete electrode model equations [2] are discretized by the finite element method (FEM) in the usual way. Using FEM we calculate approximate values of electrode voltages for the approximate element conductivity vector  $\sigma$  ( $NE \times 1$ ),  $NE$  is the number of finite elements. Furthermore, we assume the constant approximation of a conductivity distribution  $\sigma$  on the finite element region. The forward EIT calculation yields an estimation of the electric potential field in the interior of the volume under certain Neumann and Dirichlet boundary conditions. The Finite Element Method in two or

three dimensions is exploited for the forward problem with current sources. Image reconstruction of EIT is an inverse problem, which is usually presented as minimizing the suitable objective function  $\Psi(\sigma)$  relative to  $\sigma$ :

$$\min_{\sigma} \Psi(\sigma)$$

where

$$\Psi(\sigma) = \frac{1}{2} \sum \|U_M - U_{FEM}(\sigma)\|^2. \quad (2)$$

Here  $\sigma$  is the volume conductivity distribution vector in the object,  $U_M$  is the vector of measured voltages on the boundary, and  $U_{FEM}(\sigma)$  is the vector of computed peripheral voltages in respect to  $\sigma$  which can be obtained using the finite element method (FEM).

### 3. Proposed Techniques for Inverse Problem

From a mathematical perspective, the EIT inverse problem searches for parameters in a high-dimensional space. To minimize the objective function  $\Psi(\sigma)$  we can use a deterministic approach based on the Least Squares (LS) method. Due to the ill-posed nature of the problem, regularization has to be used. A heuristic approach based on suitable modification of the Differential Evolution algorithm provides another possibility of solving the EIT problem successfully.

#### 3.1 Tikhonov Regularization

First the standard Tikhonov Regularization method (TRM) described in [3] was used to solve this inverse EIT problem. So we have to minimize the objective function  $\Psi(\sigma)$

$$\Psi(\sigma) = \frac{1}{2} \sum \|U_M - U_{FEM}(\sigma)\|^2 + \alpha \|L\sigma\|^2 \quad (3)$$

where  $\alpha$  is a regularization parameter and  $L$  is a regularization matrix connecting adjacent elements of the different conductivity values. For the solution of (3) we applied the Newton-Raphson method and after the linearization we used the iteration procedure

$$\sigma_{i+1} = \sigma_i + (J_i^T J_i + \alpha L^T L)^{-1} (J_i^T (U_M - U_{FEM}(\sigma_i)) - \alpha L^T L \sigma_i) \quad (4)$$

Here  $i$  is the  $i$ -th iteration and  $J$  is the Jacobian for forward operator  $U_{FEM}$ . The Jacobian can be calculated very effectively, for example by using the reciprocity principle [4]. This iterative procedure and its improvements [5], [6] are commonly used in the EIT inverse problem for their fast convergence and good reconstruction quality. However, they are likely to be trapped in local minima and so sophisticated regularization must be taken into account to obtain the stable solution.

Applying both the described reconstruction algorithms, it is often very difficult to ensure the stability and sufficient accuracy of the required solution, because of their sensitivity to the suitable choice of the regularization parameter  $\alpha$ , as well as starting values of conductivity  $\sigma$ .

The stability of the TRM algorithm is a bit sensitive to the setting of the starting value of conductivity. The regularization parameter  $\alpha$  controls the relative weighting allocated to the prior information. Its optimal choice provides balance between the accuracy and stability of solution.

On the basis of many numerical experiments, it is supposable that we obtain higher accuracy of the reconstruction results for smaller value of the parameter  $\alpha$ , but if the value of  $\alpha$  is decreasing, the instability of the solution is increasing. In this novel approach, we search the optimal value of  $\alpha$  during the iteration procedure using the following algorithm

```

set starting variable  $\sigma$ , initialize parameter  $\alpha$ 
while
regularization is stable and
reduction of  $\Psi$  has been obtained
    use to recover optimized value of  $\sigma$ 
    decrease  $\alpha$ 
end while
    
```

In this way (TRM $\alpha$ ), we can obtain the stable solution with required higher accuracy of the reconstruction results.

#### 3.2 Differential Evolution Algorithm

Global optimizing evolutionary algorithms, such as genetic algorithms, have been recently applied to the EIT problem [7]. Some results of genetic algorithm research are described in [8]. Compared to the genetic algorithm, the differential evolution algorithm (DEA) is a relatively new heuristic approach to minimizing nonlinear and non-differentiable functions in a real and continuous space. DEA converges faster and with more certainty than many other global optimization methods according to various numerical experiments. It requires only a few control parameters and it is robust and simple in use.

The DEA maintains a population of constant size that consists of  $N$  real-valued vectors  $x_{i,G}$ ,  $i=1, 2, 3, \dots, N$ , where  $i$  indicates the index of population and  $G$  is the generation the population belongs to.

The initial population of DEA is randomly generated within the feasible range of the parameter. Subsequently, mutation is performed. For each target vector  $x_{i,G}$  a mutant vector  $v_{i,G+1}$  can be generated

$$v_{i,G+1} = x_{i,G} + \alpha_p (x_{best,G} - x_{i,G}) + \alpha_p (x_{r1,G} - x_{r2,G})$$

where  $x_{best,G}$  is the best member of the current population, random indexes  $r1, r2 \in \{1, 2, 3, \dots, N\}$  are mutually different integers, at the same time different from running in-

dex  $i$ . Parameter  $\alpha_p \in (0, 2)$  is a real constant which controls the amplification of the differential variations.

Crossover is introduced to increase the diversity of the population. New vectors are formed using random generation, permutation and replacement of randomly chosen parts of two different individuals. To decide whether or not the new vector should become a member of generation  $G + 1$ , the new vector is compared with the target vector  $x_{i,G}$ . The vector with a smaller objective function is retained in minimization. Finally, to guarantee the parameter values located inside their allowed ranges after reproduction, a simple method of replacing the parameter values that violate boundary constraints with random value generated within feasible range is used.

The evolution will be determined once the objective function reaches a predetermined value or the evolution comes to the present generations.

## 4. Simulation Results and Comparison

The following examples describe the use of the above mentioned methods for recovering a collection of linear cracks in a homogeneous electrical conductor from boundary measurements of voltages induced by specified current fluxes. To recover conductivity distributions the LS method with a different type of the regularization's way was used. Furthermore, we compare the results obtained by DEA together with the results which were recovered by the TRM $\alpha$  to different values of the regularization parameter  $\alpha$  during the reconstruction's process and the initial values of conductivity  $\sigma$ . To evaluate the quality of simulation results, the total error  $Err$  of the recovered conductivity distribution  $\sigma$  is defined as

$$Err = \sqrt{\frac{\sum_{i=1}^{NE} (\sigma(i) - \sigma_{orig}(i))^2}{\sum_{i=1}^{NE} (\sigma_{orig}(i))^2}} \cdot 100 \% \quad (5)$$

where  $\sigma_{orig}$  (in S/m) is the actual (original) value,  $\sigma$  is the value recovered by EIT.

The above proposed algorithms for 2D model have been implemented into the modification of the program [9] which has been written in MATLAB 7.0.4. Both the above described techniques have been applied to 3D model and have been implemented into a new program written in ANSYS.

### 4.1 Examples in 2D

Example of 2D arrangement for a numerical experiment is given in Fig. 1. Circle model is shown with dimensions in cm; the total number of electrodes is 20. We applied a total of 20 different cosine current excitations calculating 19 independent nodal voltages for each excitation.

Two different examples of a crack's distribution are presented. One of them is the following. In Fig. 2 you can see the FEM mesh for calculations of the gradients, voltage reference values and the Jacobians during iterations. The total number of elements is  $NE = 500$ , the number of nodes is  $NU = 271$ . We assume a homogeneous object with conductivity  $6 \cdot 10^7$  S/m on all elements except for the chosen ones where the values of conductivity are 0 S/m; on twelve colored elements in Fig. 2. These elements can represent some cracks.

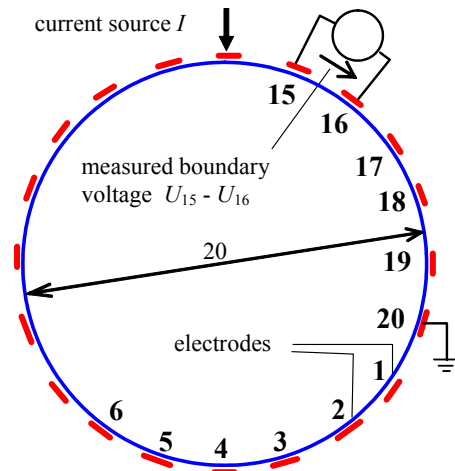


Fig. 1. An arrangement for 2D experiments.

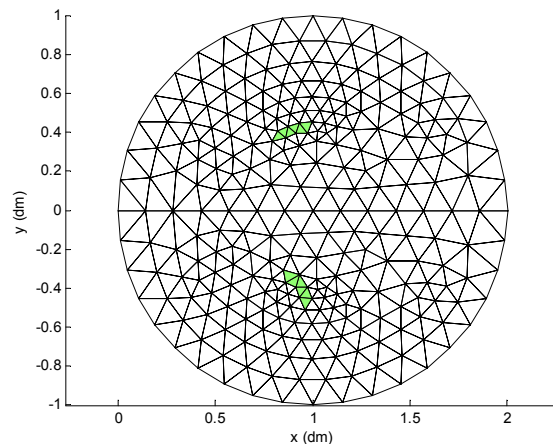


Fig. 2. FEM grid and elements with non-homogeneity.

The recovered conductivity distribution obtained using TRM $\alpha$  is shown in Fig. 3 and using DEA with number of generations  $G = 60$  is shown in Fig. 4.

Another example of the crack's distribution is in Fig. 5 and experimental results are shown in Fig. 6 and Fig. 7.

The starting and final values of parameter  $\alpha$ , primal objective function  $\Psi(\sigma)$ , and total error  $Err$  are given in Tab. 1 – example 1 and in Tab. 2 – example 2.

The suitable choice of starting value of parameter  $\alpha$  is necessary to assure the stability of the reconstruction process using TRM $\alpha$ .

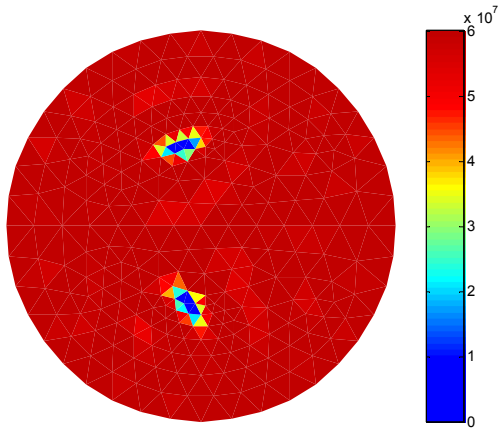


Fig.3. Final conductivity distribution obtained using TRMα.

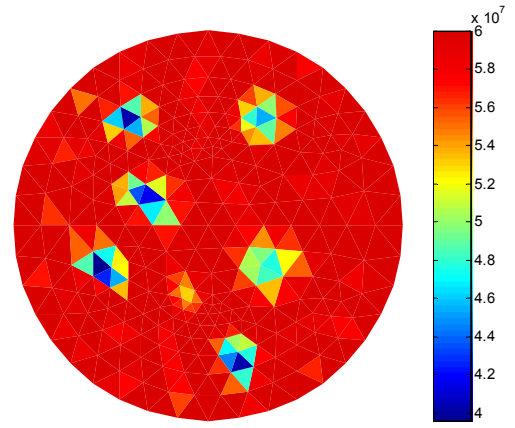


Fig.6. Final conductivity distribution obtained using TRMα.

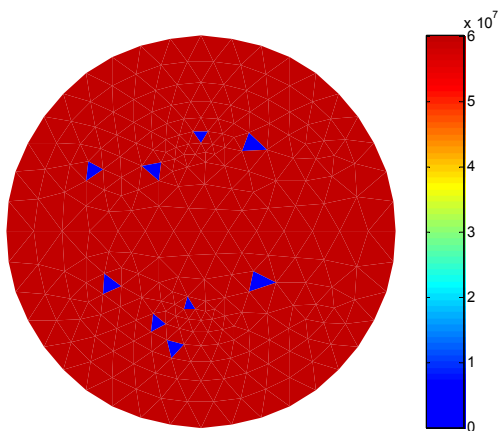


Fig.4. Final conductivity distribution obtained using DEA.

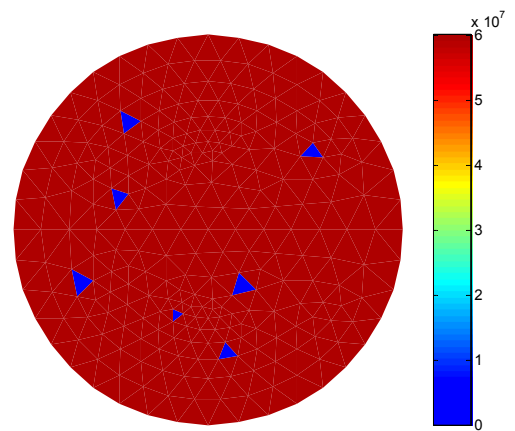


Fig.7. Final conductivity distribution obtained using DEA.

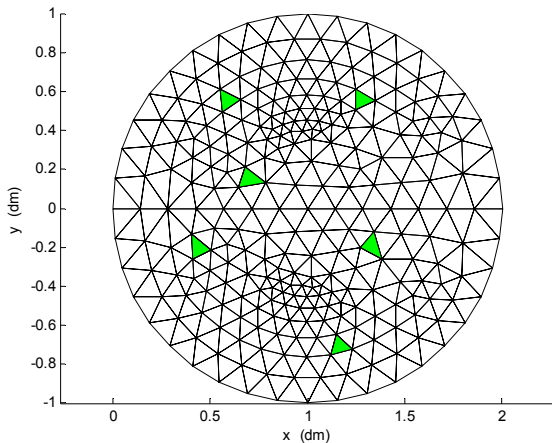


Fig.5. FEM grid and elements with non-homogeneity.

|                           | TRM                | TRMα               | DEA                |
|---------------------------|--------------------|--------------------|--------------------|
| $\alpha$ , starting       | $5 \cdot 10^{-40}$ | $5 \cdot 10^{-40}$ | -                  |
| $\alpha$ , final          | $5 \cdot 10^{-40}$ | $1 \cdot 10^{-45}$ | -                  |
| $\Psi(\sigma)$ , starting | $2 \cdot 10^{-17}$ | $2 \cdot 10^{-17}$ | $5 \cdot 10^{-14}$ |
| $\Psi(\sigma)$ , final    | $1 \cdot 10^{-17}$ | $8 \cdot 10^{-18}$ | $3 \cdot 10^{-19}$ |
| Err, starting             | 30%                | 30%                | 27%                |
| Err, final                | 22%                | 9%                 | 11%                |

Tab. 1. Comparison of recovered results for example 1.

## 4.2 Examples in 3D

There is an FEM grid with 570 nodes, 432 elements and 40 electrodes in Fig. 8. The radius of the cylinder is 10 cm, its height is 20 cm. We applied a total of 40 different current excitations calculating 39 independent nodal voltages for each excitation.

|                           | TRM                | TRMα               | DEA                |
|---------------------------|--------------------|--------------------|--------------------|
| $\alpha$ , starting       | $5 \cdot 10^{-40}$ | $5 \cdot 10^{-40}$ | -                  |
| $\alpha$ , final          | $5 \cdot 10^{-40}$ | $4 \cdot 10^{-43}$ | -                  |
| $\Psi(\sigma)$ , starting | $5 \cdot 10^{-18}$ | $5 \cdot 10^{-18}$ | $5 \cdot 10^{-14}$ |
| $\Psi(\sigma)$ , final    | $1 \cdot 10^{-18}$ | $3 \cdot 10^{-19}$ | $7 \cdot 10^{-20}$ |
| Err, starting             | 35%                | 35%                | 27%                |
| Err, final                | 25%                | 11%                | 10%                |

Tab. 2. Comparison of recovered results for example 2.

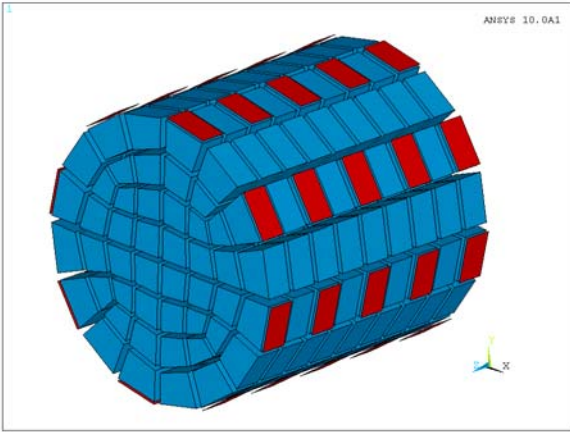


Fig. 8. FEM grid and the position of electrodes for 3D testing.

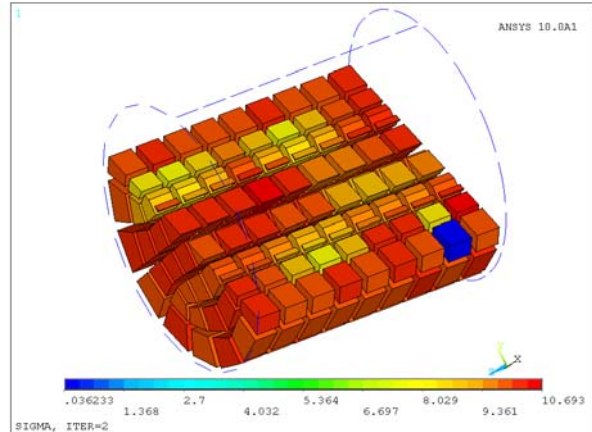


Fig. 10. Conductivity distribution after 2 iterations.

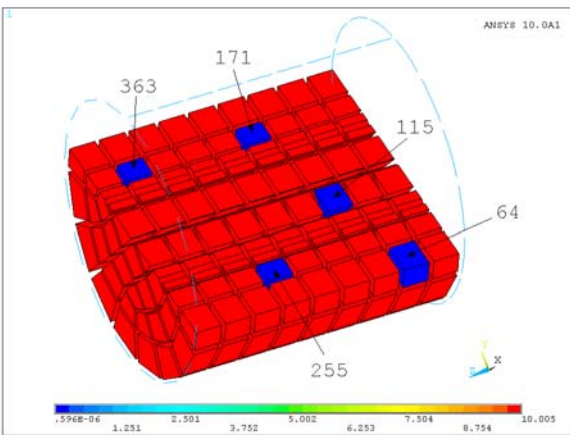


Fig. 9. Five selected elements with non-homogeneity.

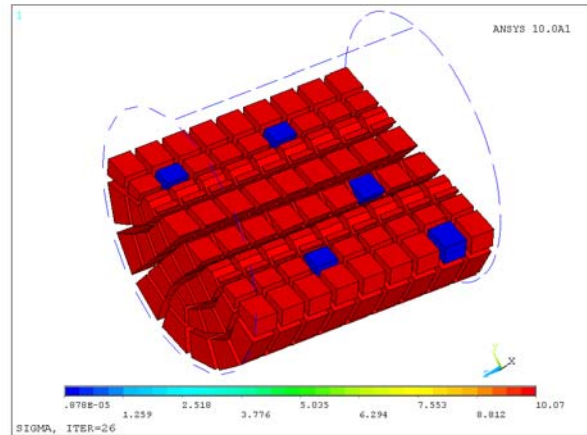


Fig. 11. Final conductivity distribution obtained using TRMα.

We assume homogeneous object with conductivity 10 S/m on all elements except for the chosen ones where values of conductivity (on five blue color marked elements in Fig. 9) are 0 S/m. These elements can represent some cracks.

An example of the reconstruction results, using Tikhonov regularization with optimized value of the parameter  $\alpha$ , is given in Fig. 10 and Fig. 11. The starting values of conductivity are 8 S/m on all elements; the starting value of parameter  $\alpha$  is  $1 \cdot 10^{-10}$  and its final value is  $0.3 \cdot 10^{-17}$ . The conductivity distribution after 2 iterations is shown in Fig. 10 and the final conductivity distribution after 30 iterations in Fig. 11.

The conductivity changes on the elements with non-homogeneities during the iteration process are shown in Fig. 12. The final value of the primal objective function  $\Psi(\sigma)$  is  $5.3 \cdot 10^{-39}$  and the total error  $Err$  is 0.01 %.

To recover the conductivity distribution according to Fig. 9 we also use the differential evolution algorithm.

Experimental results are shown in Fig. 13; here you can see the starting values of the conductivity distribution. The final values of the recovered conductivity of the best member of 207 generation are shown in Fig. 14. The final value of the primal objective function  $\Psi(\sigma)$  is  $2.8 \cdot 10^{-14}$  and the total error  $Err$  is 16 %.

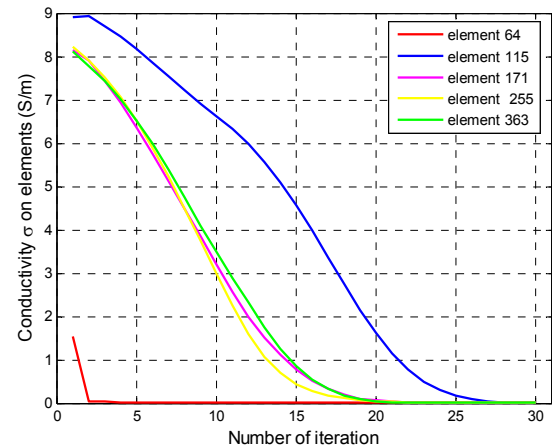


Fig. 12. Conductivity changes on non-homogeneities.

## 5. Conclusions

In this paper, a new practical approach to the reconstruction of non-homogeneities using EIT has been presented. Many numerical experiments performed during the above described research have resulted in the conclusion that the applications of the TRMα and DEA reconstruction algorithm have an advantage over the TRM approach. We

mostly obtain higher accuracy using the TRM $\alpha$  but there is often an unstable reconstruction process. On the other hand the results obtained using DEA are less accurate but there is always a stable process. All the results stated above as well as many other examples were obtained using a program written in MATLAB for 2D reconstruction and in ANSYS for 3D reconstruction by the authors.

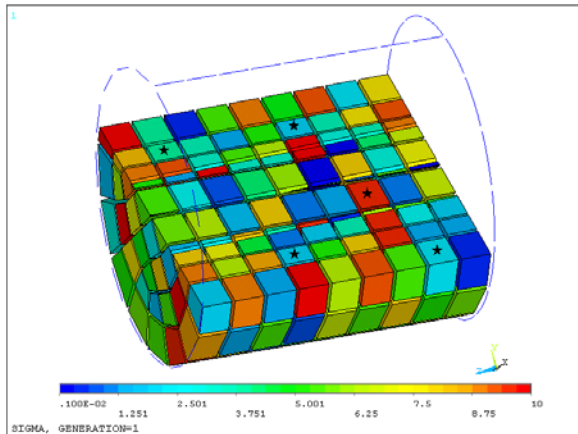


Fig.13. Starting values of a conductivity distribution.

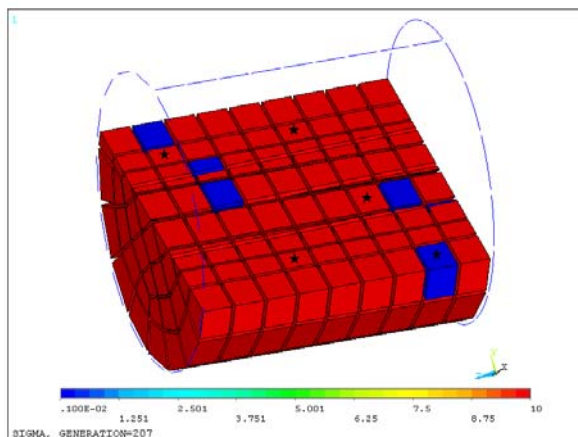


Fig. 14. Final conductivity distribution obtained using DEA.

It would be very worth to try another new ways of an effective and an absolutely stable reconstruction of the conductivity distribution with the highest accuracy. It can be tested for example an apposite combination of certain heuristic technique with the widely known method Total Variation Primal Dual-Interior Point Method [9], methods based on Genetic Algorithm, Level Set Method [10] etc.

## Acknowledgements

The research described in the paper was financially supported by the research program MSM 0021630513.

## References

- [1] CHENEY, M., ISAACSON, D., NEWELL, J., C. Electrical impedance tomography. *SIAM Rev.*, vol. 41, no. 1, 1999, p. 85-101.
- [2] SOMERSALO, E., CHENEY, M., ISAACSON, D. Existence and uniqueness for electrode models for electric current computed tomography. *SIAM J. Appl. Math.*, vol. 52, 1992, p. 1023-1040.
- [3] VAUHKONEN, M., VADÁSZ, D., KARJALAINEN, P. A., SOMERSALO, E., KAIPIO, J. P. Tikhonov regularization and prior information in electrical impedance tomography. *IEEE Trans. Med. Eng.*, 1998, vol. 17, p. 285-293.
- [4] BRANDSTÄTTER, B. Jacobian calculation for electrical impedance tomography based on the reciprocity principle. *IEEE Transaction on Magnetics*, 2003, vol. 39, no. 3, p.1309-1312.
- [5] YORKEY, T. J., WEBSTER, J. G., TOMKINS, W. J. Comparing reconstruction algorithms for electrical impedance tomography. *IEEE Trans. Biomed. Eng.*, 1987, vol. 34, p. 843-852.
- [6] RAO, L., HE, R., WANG, Y., YAN, W., BAI, J., YE, D. An efficient improvement of modified Newton-Raphson algorithm for electrical impedance tomography. *IEEE Transaction on Magnetics*, 1999, vol. 35, p. 1562-1565.
- [7] OLMI, R., BINI, M., PRIORI, S. A genetic algorithm approach to image reconstruction in electrical impedance tomography. *IEEE Trans. Evol. Comp.*, 2000, vol. 4, p. 83-88.
- [8] MICHALEWICZ, Z. Genetic algorithms+Data Structure=Evolution Programs. 2<sup>nd</sup> ed. Springer Verlag Berlin, 1994.
- [9] BORSIC, A. Regularization methods for imaging from electrical measurement. PhD. Thesis, Oxford Brookes University, 2002.
- [10] BURGER, M. A level set method for inverse problems, *Inverse Problems* 17, 2001, p. 1327-1356.

## About Authors...

**Tibor BACHOREC** was born in 1969 in Slovakia. He received his master's degree in electrical engineering from Brno University of Technology in 1993. He is interested in numerical methods, especially FEM, used for an analysis of different cases of physical fields. His research is focused on regularization techniques for inverse problems.

**Jarmila DĚDKOVÁ** was born in 1959 in Znojmo. She received her master's degree in electrical engineering from Brno University of Technology in 1983. Her professional and current research interests are in the development of programs for the electromagnetic field modeling, optimization and effective solutions of inverse problems.